Article

Influence of Dynamic Power Compensation in an Isothermal Titration Microcalorimeter

Luis Garca-Fuentes, Carmen Barn, and Obdulio L. Mayorga

Anal. Chem., **1998**, 70 (21), 4615-4623 • DOI: 10.1021/ac980203u

Anal. Chem. **1998,** *70,* 4615−4623

Influence of Dynamic Power Compensation in an Isothermal Titration Microcalorimeter

Luis García-Fuentes,*,†,‡ Carmen Barón,†,‡ and Obdulio L. Mayorga‡

Departamento de Química Física, Bioquímica y Química Inorgánica, Facultad de Ciencias Experimentales, Universidad de Almería, Almería, Spain, and Instituto de Biotecnología de la Universidad de Granada, Granada, Spain

A theoretical analysis in Laplace's transformed domain based on a power balance represents a suitable model for an isothermal titration calorimeter with dynamic power compensation, designed and implemented in our laboratory. A rigorous calibration of the injection system and the calorimetric response was also made. Using electrically generated heat pulses, two different time constants have been determined from the calorimetric transfer function and assigned to the physical parts of the calorimeter. The same was done for a protein−ligand interaction. The binding of 2′-CMP to ribonuclease A at low and high ionic strengths was used to check the apparatus and the results were compared with those obtained by other authors (Wiseman, T.; Williston, S.; Brandts, J. F.; Lung-Nan, L. *Anal. Biochem.* 1989, *179*, 131−137). In this case, the analysis showed a different time constant for the heat source. Independently of the nature of the heat source, the calorimetric time constants obtained while working under compensation are always smaller than those corresponding to a noncompensated system. The improvement of the calorimetric response introduced by dynamic power compensation is thus explained in terms of the reduction of the time constants characteristic of the calorimeter. This theoretical model can be used to predict the shape of the thermogram for any given reaction of either known or supposed thermodynamic parameters. Therefore, the calorimetric study is extended to the other nucleotides, 2′-UMP and 5′-dUMP, which have not hitherto been reported in the literature.

In 1990, Freire et al. published a review on the technological advances and development of isothermal titration calorimetry (ITC) applications to biomedical research, in which they described some applications of this technique to systems of biological interest.[1] The main conclusion in their report was that the development of high-sensitivity titration calorimeters had opened the way to the direct thermodynamic characterization of many biological systems. Since then, thanks mainly to the commercial availability of the MicroCal Omega titration calorimeter,[2] its biological applications have increased significantly. Some that we might add to those already mentioned[1] encompass such aspects as combined crystal structure and ligand binding studies,[3,4] antigen−antibody interactions,[5,6] protein−carbohydrate interactions,[7] thermodynamic approaches to the molecular recognition of drugs and other applications in the pharmaceutical sciences,[8,9] and studies of the interaction between drugs and living cell systems.[10,11] Nevertheless, for protein−ligand or protein−protein interactions with extremely small enthalpy changes, it is essential to achieve a more acute sensitivity than that currently available because, although genetic engineering provides us now with larger quantities of samples, the amounts and concentrations of proteins or ligands required to carry out an experiment may still be prohibitively high. Thus, technological improvements must be made to the current generation of microcalorimeters in order to improve their sensitivity. For example, better and faster temperature sensors than the semiconductor thermopiles in common use today are necessary. More sophisticated designs of the microcalorimetric unit, especially the reaction cells, would also contribute to an increase in their sensitivity. But in addition to these hoped-for technological advances, methodological innovations can also improve the characteristics and useful application of isothermal titration calorimeters, especially, for example, with regard to the use of compensation methods to measure the thermal effects. McKinnon et al.[12] and Freire et al.[1] have reported how such compensation mechanisms decrease the response time of the ITC and at the same time improve the signal-to-noise ratio or, in other words, increase the sensitivity of the instrument. Dynamic power compensation in ITC is based in the principles of general response theory. From this approach, the response of a calorimeter to a given thermal effect is determined by its transfer

* To whom correspondence should be adressed: Departamento de Química Física, Bioquímica y Química Inorgánica, Facultad de Ciencias Experimentales, Universidad de Almería, La Cañada de San Urbano s/n, 04120 Almería, Spain. Telephone: 34-950-215618. Fax: 34-950-215008. E-mail: lgarcia@ualm.es.

† Universidad de Almería.

‡ Universidad de Granada.

(1) Freire, E.; Lopez-Mayorga, O.; Straume, M. *Anal. Chem.* **1990**, *62*, 950−958.

(2) Wiseman, T.; Williston, S.; Brandts, J. F.; Lung-Nan, L. *Anal. Biochem.* **1989**, *179*, 131−137.

(3) Weber, P. C.; Pantoliano, M. W.; Thompson, L. D. *Biochemistry* **1992**, *31*, 9350−9354.

(4) Connelly, P. R.; Aldape, R. A.; Bruzzese, F. J.; Chambers, S. P.; Fitzgibbon, M. J.; Fleming, M. A.; Itoh, S.; Livingston, D. J.; Navia, M. A.; Thomson, J. A.; Wilson, K. P. *Proc. Natl. Acad. Sci. U.S.A.* **1994**, *91*, 1964−1968.

(5) Ito, W.; Kurosawa, Y. *J. Biol. Chem.* **1993**, *268*, 16639−16647.

(6) Ito, W.; Kurosawa, Y. *J. Biol. Chem.* **1993**, *268*, 20668−20675.

(7) Chervenak, M. C.; Toone, E. J. *Biochemistry* **1995**, *34*, 5685−5695.

(8) Buckton, G. *Thermochim. Acta* **1995**, *248*, 117−129.

(9) Aki, H.; Goto, M.; Yamamoto, M. *Thermochim. Acta* **1995**, *251*, 379−388.

(10) Wadsö, I. *Thermochim. Acta* **1995**, *267*, 45−59.

(11) Wadsö, I. *Thermochim. Acta* **1995**, *270*, 337−350.

(12) McKinnon, I. R.; Fall, L.; Parody, A.; Gill, S. J. *Anal. Biochem.* **1984**, *139*, 134−139.

10.1021/ac980203u CCC: $15.00
Published on Web 10/02/1998

function. This function contains all necessary information to predict the behavior of the system and can be modified by positive or negative signal feedback. The static and dynamic characteristics of any heat conduction calorimeter are improved by negative feedback.

Our aim here is to explain formally our empirical results through the development of a theoretical model that adequately represents the instrument. The capacity to predict correctly the response of the calorimeter to any given thermal effect would allow us to optimize the experiments, as well as to widen the field of applications. Thus, for example, if on the basis of an acceptable model the transfer function of the calorimeter were experimentally determined, it would be possible to obtain kinetic information from dynamically corrected thermograms.[13]

The purpose of our study into ribonuclease−nucleotide interactions is a dual one: on one hand, some of these binding reactions have already been well characterized thermodynamically by calorimetric methods (see below), and, therefore, these are suitable reactions to check the performance of our microcalorimeter, while on the other hand, the corresponding thermograms are used as input datasets for the experimental determination of the calorimeter transfer function.

EXPERIMENTAL SECTION

Chemicals. Bovine pancreatic ribonuclease A was purchased from Boehringer Mannhein Corp. and used without further purification. The concentrations of ribonuclease A were determined from absorbance measurements at 277.5 nm, assuming a molar absorption coefficient of 9800 M^{-1} cm^{-1}. 2′-Cytidine monophosphate (2′-CMP), 2′-uridine monophosphate (2′-UMP), and 2′-deoxyuridine-5′-monophosphate (5′-dUMP), of the highest purity available, were all bought from Sigma and used without any further purification. Two protein solutions at "high" and "low" ionic strengths[2] were prepared by dissolving the protein in either 0.2 M KAc and 0.2 M KCl at pH 5.5 or 50 mM NaAc at pH 5.5. Both solutions were dialyzed at 4 °C against the corresponding acetate buffer for 12 h with two changes of buffer. The concentrations of 2′-CMP, 2′-UMP, and 5′-dUMP were determined from absorbance measurements at 260 nm in 100 mM KH_2PO_4, pH 7, using molar absorption coefficients of 7400, 10^4, and 10^4 cm^{-1} M^{-1}, respectively. All other chemicals were of the highest purity available.

Instrumentation. *Configuration and Implementation of the Calorimeter.* Our titration microcalorimeter was built on the principle of a fully symmetrical configuration (Figure 1). In this arrangement, known as a differential or twin calorimeter,[14] two reaction cells, S and R, are placed into identical slots of a large aluminum block, B. The large heat capacity of this block provides sufficient thermal inertia to act as a heat sink and to be temperature controlled to within 1 mK. The two cylindrical cells were made as identical as possible and have a large base area-to-thickness ratio. They are made from gold, which has two essential properties: good thermal conductivity and considerable chemical inertia toward the biochemical systems under study. One cell acts as the reaction vessel (the sample cell, S) and the other as the reference cell (R). The injection and stirring systems are also symmetrical; thus, the assignment of the cells as sample and reference is completely arbitrary.

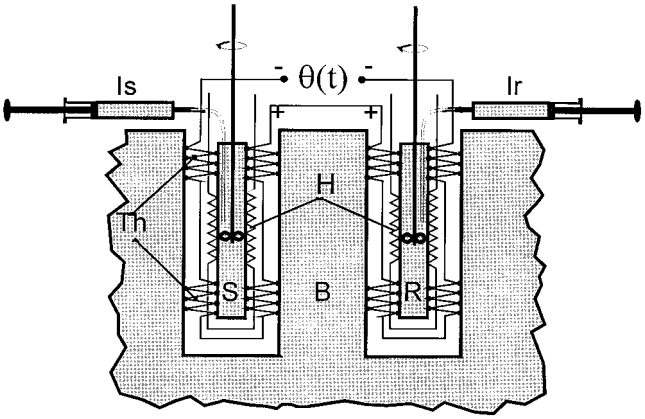

Figure 1. Configuration of the isothermal titration calorimeter. S, sample cell; R, reference cell; B, heat sink; Th, semiconductor thermopiles; H, electrical heater; Is, sample microsyringe; Ir, reference microsyringe.

Different types of experiments can be carried out: stepwise titration may be performed, for example, by filling the sample cell with the solution of the reagent to be titrated and the reference cell with buffer. The microsyringe of the sample cell, Is (see Figure 1), is filled with a solution of the titrant reagent and that of the reference cell, Ir, with the buffer. After a time lapse to allow thermal equilibration, a sequence of identical injections of small volume (5−30 μL) are simultaneously made into both cells. Most of the physical effects common to both cells, including heat leakage, are compensated for. Blank experiments, filling the sample cell with buffer, can be made to evaluate thermal effects which are not common to both cells but are concomitant with the heats of reaction.

The temperature sensor, an assembly of MELCOR FC0.45-66-05L semiconductor (bismuth telluride) thermopiles with a high density of junctions (Th in Figure 1), is the only fastening to hold the cell in place. Therefore, if we dismiss as negligible the heat transported by air convection and radiation, most of the heat generated flows by conduction through the thermopiles to the block of the calorimeter. A small amount of heat does, nevertheless, leak through the stirrers, tubing, and cables. But chemical and/or electrical calibrations under the same experimental conditions allow us to correct this heat leak, and the measurement of the thermal effect thus becomes highly accurate. If any heat is released or is absorbed in a cell, the temperature difference between the cell and the heat sink will be a slowly evolving function of time, $\Delta T(t)$; the assembly of thermopiles will generate an electromotive force function $E(t) = k\Delta T(t)$, where k is the Seebeck constant of this temperature sensor. Moreover, for small values of $\Delta T(t)$, a signal slowly evolving in time, Newton's law of cooling is obeyed closely enough:

$$\frac{dQ(t)}{dt} = W(t) = \alpha\Delta T(t) \Rightarrow W(t) = \frac{\alpha}{k}E(t) = \epsilon E(t) \quad (1)$$

where $Q(t)$ is the heat generated, α is a global coefficient of heat exchange, and $\epsilon = \alpha/k$.

The thermopiles for both cells are assembled identically and are connected in opposition. Thus, the electrical signal generated

(13) López-Mayorga, O.; Freire, E. *Biophys. Chem.* **1987**, *87*, 87−96.
(14) Hemminger, W.; Höhne G. *Calorimetry. Fundamentals and Practice*; Verlag Chemie: Weinheim, Germany, 1984.

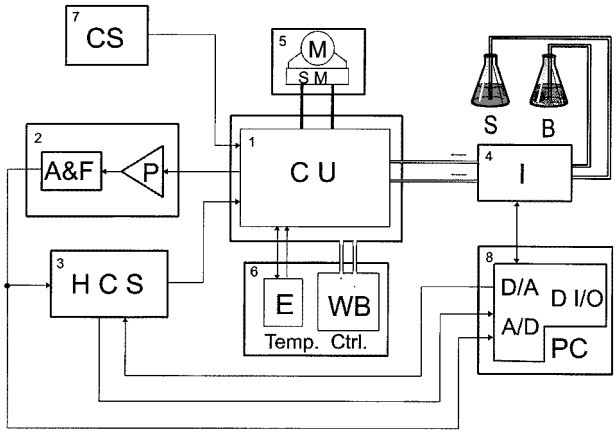

Figure 2. Block diagram of the calorimetric system. Box 1: CU, calorimetric unit. Box 2: P, preamplifier; A&F, amplifier and filter. Box 3: HCS, heat compensation system. Box 4: I, injection controller. Box 5: M and SM, motor and stirring mechanism, respectively. Box 6: Temp. Ctrl., temperature controller; WB, water bath; E, electronic temperature controller. Box 7: CS, current source for electrical calibration. Box 8: PC, personal computer; D/A, digital-to-analog converter; A/D, analog-to-digital converter; D I/O, digital input−output.

by any thermal effect is proportional to the difference between the heat exchange rates between the cells and the sink as well as to the temperature difference between the cells themselves:

$$\Delta E(t) = E_{SC} - E_{RC} = k[T_{SC}(t) - T_{RC}(t)] = k\theta(t) \quad (2)$$

where E_{SC} and E_{RC} are the electromotive forces generated by the thermopiles of the sample and reference cells, respectively, and $\theta(t) = T_{SC}(t) - T_{RC}(t)$ is the temperature difference between the cells. The heat effect is compensated for by a negative feedback system that uses $\theta(t)$ as the error signal and two coils of high-resistance wire (H in Figure 1) as heaters. Any thermal effect obliges the feedback system to produce an opposite effect on the background heat; thus, $\theta(t)$ is always close to zero.

Some electronic devices and other accessories are necessary to run the calorimeter. A block diagram of the total system appears in Figure 2; CU (box 1) symbolizes the calorimetric unit just described above. The signal $\Delta E(t)$, only a few microvolts at most, is amplified to hundreds of millivolts and filtered to some slight degree by the electronic device represented by box 2. The heat compensation system (HCS, box 3) is an electronic circuit which compensates in real time for the thermal effect and generates a signal proportional to the compensated heat. This signal and the amplified/filtered $\Delta E(t)$ are digitalized by a data acquisition system (Data Translation, DT2805) interfaced to a personal computer with a 486DX2 or higher Intel microprocessor. Temperature stability, better than 2.5×10^{-3} °C h^{-1}, must be achieved to minimize the slow fluctuations of the baseline that limit the sensitivity of the calorimeter. For this requirement, an electronic proportional temperature controller (E, box 6) operates directly on the thermal sink, and the entire calorimetric unit is surrounded by a metal jacket through which thermostated water from an external bath (WB, box 6) circulates. Two Hamilton syringes (250 μL each) attached to a sliding mechanism make up a very precise and highly accurate injection device (I, box 4). A stepping motor of 200 steps/turn with a coupled micrometric screw (0.5 mm/turn) drives the mechanism under computerized digital control. Finally, a stirring mechanism (M/SM, box 5) and a regulated current source (CS, box 7) for electrical calibration completes the general calorimetric system. All electronic devices—preamplifier, amplifier/filter, proportional temperature controller, current and voltage sources, injection controller, etc.—were designed and built in our laboratory.

Calibrations of Instrument. To obtain a reliable quantitative measurement, the injection system and the calorimetric response must be carefully calibrated. The injection system consists of two microsyringes driven by a stepping motor digitally controlled by a computer. With a different number of motor steps, several injections of Milli Q water were made at the working temperature of 25 °C, and the volume was calculated by weighing the injected water and taking into account a water density of $\rho(25\ °C) = 0.99707$ g mL^{-1}. Linear regression of the total set of data provided by both syringes gives an injection calibration parameter of $\phi = 0.0104 \pm 0.0001$ μL/step, and no systematic deviation was to be found in either syringe. This value is used temporarily by the control software until a new calibration operation is carried out.

We use the term "calibration of calorimetric response" to mean the process of obtaining the function that correlates the heat flow produced by a given thermal effect with the measured electrical signal. Working with biological systems, the thermal effects are always very small and fall within a range which fulfils a linear relationship. Thus, the calibration operation of the calorimetric signal is reduced to obtain a simple constant. In ITC, the most efficient way of establishing this constant is in terms of the ratio of heat generated to the area under the observed peak. The calibration can be made electrically and/or chemically. Joule's effect is used for the former method, feeding the calibration heater (a resistance in close contact with the calorimetric cell) with an electrical current; the accuracy of this calibration operation will depend on the accuracy with which the current, the resistance of the heater, and the warming time are determined. This calibration must be made under the same experimental conditions as the final experiment, and so it will have to be subject to the same temperature and the cells filled with the same solvent, and so on. Chemical calibration is carried out by detecting the heat of a chemical reaction, the change of enthalpy (ΔH) of which is well-known, and with not too small a rate constant (above 1 s^{-1}). Thus, the reaction of H_2O formation by the neutralization of NaOH with HCl is frequently used because of its high enthalpy change, $\Delta H(25\ °C) = -55.76$ kJ mol^{-1}.[15] Nevertheless, this exothermal reaction is too energetic for calibrating the instrument in the region of the lower heats, which are of greater biological interest, and other reactions with a smaller ΔH should be used. Protonation of the carboxylic group of glycine, which presents a $\Delta H = -4.39$ kJ mol^{-1} and a $pK_a = 2.36$,[15] is suitable for this purpose. The correlation of electrically and chemically produced heats with the areas of the corresponding peaks is within experimental error, the standard deviation being less than 2%.

Calorimetric Titration Experiment. A normal titration experiment is carried out by introducing the protein solution into the sample cell and filling the injection tube of the same cell with

(15) Christensen, J. J.; Hansen, L. D.; Izatt, R. M. *Handbook of proton ionization heats and related thermodynamic quantities*; John Wiley & Sons: New York, 1976.

ligand solution. The reference cell and its injection tube are filled with the buffer. After doing this, some time must be allowed to elapse for the system to arrive at thermal stability and thus obtain a stable baseline (usually between 60 and 90 min). Once the calorimeter gives us a stable signal, a sequence of injections of a few microliters each, spaced about 3 min apart, is begun. The recorded thermogram consists of a series of peaks, and the heat produced with each one, measured by integration, corresponds to the global heat released or absorbed at each stage of the reaction.

Two blank experiments are usually necessary to detect and measure the dilution heats. These measurements of dilution heat are carried out under the same titration conditions, except that the ligand solution in the first blank and the protein solution in the second blank are replaced by buffer. Therefore, the thermal effects associated with the dilution of the protein and ligand can be obtained independently. The net heats of the binding reaction are obtained by subtracting the corresponding dilution heats from the overall heats.

Analysis of Calorimetric Titration Data. It is assumed that a protein has m identical and independent sites for binding the ligand, L, with its characteristic microscopic association constant, K, and molar enthalpy change of binding ΔH_b, and with n_{H^+} being the number of protons taken up by the protein−ligand complex during the binding reaction. In a series of injections of ligand solution into the cell containing the protein, the heat released or absorbed for each injection, Q_{inj}, should be proportional to the increase in the saturation fraction, ΔY, associated with the change in bound ligand concentration, according to the equation

$$Q_{inj} = mV[P](\Delta H_b + n_{H^+}\Delta H_i)\Delta Y \quad (3)$$

where [P] stands for the protein concentration in the calorimeter cell, V for the reaction volume, and ΔH_i for the heat of buffer ionization. Because the sample volume, V, increases in each injection, the protein concentration, [P], decreases throughout the titration, although the number of moles of protein ([P] V) is always kept constant. In eq 3, it can be seen that the binding enthalpy does not include the enthalpy of buffer ionization but that ΔH_b retains contributions from the ionization enthalpies of groups on the protein and/or the ligand.

The dependence of the heat effect per mole of protein, ΔH_T, on the total amount of ligand added can be obtained from eq 3 and expressed as a function of the apparent microscopic association constant, K, and the free ligand concentration [L]:

$$\Delta H_T = m(\Delta H_b + n_{H^+}\Delta H_i)\frac{K[L]}{1 + K[L]} \quad (4)$$

If a buffer is used with a little ionization heat (in our case acetate, $\Delta H_i = 0.49$ kJ mol^{-1}),[15] the thermal correction for the ionization buffer ($n_{H^+}\Delta H_i$) can be negligible. A nonlinear, least-squares fitting of the experimental data in the form of the heat of individual injections (eq 3) or the cumulative heat (eq 4) allows us to estimate m, ΔH_b, and K. In any case, in an ITC experiment, only the total ligand concentration, $[L]_T$, and the total protein concentration, [P], are known. The free ligand concentration after each injection must be calculated from these according to[1]

$$[L] = \{\sqrt{(1 - K[L]_T + mK[P])^2 + 4K[L]_T} + K[L]_T - mK[P] - 1\}/2K \quad (5)$$

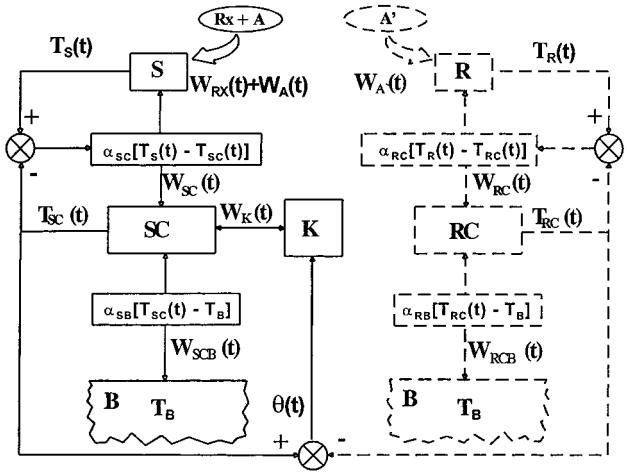

Figure 3. Diagram of heat flow in the calorimeter. S, sample solution; R, reference solution; SC, sample cell−thermopiles set; RC, reference cell−thermopiles set; K, feedback system; B, heat sink; Rx + A, chemical reaction and accidental events; $T_S(t)$, $T_R(t)$, $T_{SC}(t)$, and $T_{RC}(t)$, time functions of temperature for sample, reference, sample cell, and reference cell, respectively; T_B, temperature of heat sink; $W_{RX}(t)$, heat flow for chemical reaction; $W_A(t)$, heat flow for accidental events; $W_{SC}(t)$, heat flow between sample solution and cell; $W_{RC}(t)$, heat flow between reference solution and cell; $W_K(t)$, heat flow between feedback system an sample cell; $W_{SCB}(t)$, heat flow between sample cell and heat sink; and $W_{RCB}(t)$, heat flow between reference cell and heat sink; α_{SC}, α_{RC}, α_{SB}, and α_{RB}, coefficients of heat exchange between sample solution and cell, reference solution and cell, sample cell and heat sink, and reference cell and heat sink, respectively; $\theta(t)$, temperature difference between sample and reference cell.

RESULTS AND DISCUSSION

Model of the Calorimeter. For small thermal effects, the calorimeter can be considered as being a strictly linear system, and so it can be represented by a differential equation with constant coefficients. Thus, in a process with heat compensation, illustrated by the diagram in Figure 3, the power balance for the sample and reference solution can be described by the following equations:

$$C_S\frac{dT_S(t)}{dt} + \alpha_{SC}[T_S(t) - T_{SC}(t)] = W_{RX}(t) + W_A(t) \quad (6)$$

$$C_R\frac{dT_R(t)}{dt} + \alpha_{RC}[T_R(t) - T_{RC}(t)] = W'_A(t) \quad (7)$$

where C_S and C_R are the heat capacity of the sample and the reference substance, $T_S(t)$, $T_R(t)$, $T_{SC}(t)$, and $T_{RC}(t)$ are the time-dependent temperature functions for the sample and reference solutions and the sample and reference cells, respectively, α_{SC} is the coefficient of heat exchange between the sample solution and sample cell, and α_{RC} is the same coefficient for the reference side

of the system. Finally, $W_{RX}(t)$ symbolizes the heat flow from the chemical reaction taking place in the sample cell, while $W_A(t)$ and $W_A'(t)$ represent the heat flows produced by accidental phenomena in each of the cells.

Similarly, the balance of power for each cell and its control components, i.e., the thermopiles (Th) and the heaters (H), can be expressed by the two following equations:

$$C_{SC}\frac{dT_{SC}(t)}{dt} + \alpha_{SB}[T_{SC}(t) - T_B(t)] = \alpha_{SC}[T_S(t) - T_{SC}(t)] + W_K(t) \quad (8)$$

$$C_{RC}\frac{dT_{RC}(t)}{dt} + \alpha_{RB}[T_{RC}(t) - T_B(t)] = \alpha_{RC}[T_R(t) - T_{RC}(t)] \quad (9)$$

where C_{SC} and C_{RC} now stand for the heat capacity of the sample and reference cells, T_B is the temperature of the heat sink, and α_{SB} and α_{RB} are the coefficients of heat exchange between the cells and the heat sink. The term $W_K(t)$ in eq 8 represents the heat flow governed by the feedback system on the sample cell.

If we accept the approximations $W_A(t) \cong W_A'(t)$, $\alpha_{SB} \cong \alpha_{RB}$, and $\alpha_{SC} \cong \alpha_{RC}$ to be valid, the following differential equation of the variable $\theta(t)$ can be deduced by combining eqs 6−9:[16−18]

$$W_{RX}(t) + W_K(t) = \alpha_{SB}\theta(t) + (\alpha_{SC} + \alpha_{SB})\left[(\tau_S + \tau_C)\frac{d\theta(t)}{dt} + \tau_S\tau_C\frac{d^2\theta(t)}{dt^2}\right] \quad (10)$$

where τ_S and τ_C are the thermal relaxation times of sample and calorimetric cells, respectively.

$$\tau_S = \frac{C_S}{\alpha_{SC}}, \quad \tau_C = \frac{C_{SC}}{\alpha_{SC} + \alpha_{SB}} \quad (11)$$

For a given function for $W_{RX}(t)$, differential eq 10 must be solved. The modeling of the system is greatly simplified, however, if we carry out the analysis in Laplace's transformed domain.[19−22] Following this approach, each component of the system is represented by its corresponding transfer function in the domain of the complex variable $s = \sigma + jw$ (w being the angular frequency, σ a convergence factor, and $j = (-1)^{1/2}$). The sample, the reference, the sample cell, the reference cell, and the feedback transfer functions being indicated by $S(s)$, $R(s)$, $SC(s)$, $RC(s)$ and $K(s)$, the diagram in Figure 3 can be reduced to the diagram shown on the left-hand side of Figure 4.

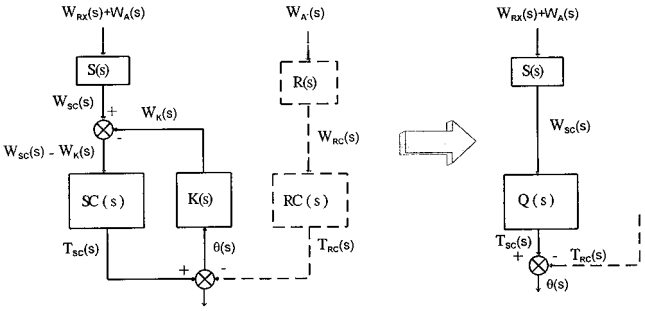

Figure 4. Diagram of heat flow in the Laplace domain. Left: $S(s)$, $R(s)$, $SC(s)$, $K(s)$, and $RC(s)$, transfer functions for sample solution, reference solution, sample cell, feedback system, and reference cell, respectively. $W_{RX}(s)$, $W_A(s)$, $W_{SC}(s)$, $W_{RC}(s)$, and $W_K(s)$, Laplace transforms of heat flows indicated in the Figure 3. $T_{SC}(s)$, $T_{RC}(s)$, and $\theta(s)$, Laplace transforms of $T_{SC}(t)$, $T_{RC}(t)$, and $\theta(t)$, respectively. Right: Simplified block diagram; $Q(s)$, equivalent transfer function of the combined SC−K block.

Taking each component to be a first-order subsystem, these transfer functions will take the form

$$X(s) = \frac{A}{1 + \tau_X s} \quad (12)$$

where X is any of the above-mentioned transfer functions, and A is a constant that is equal to 1 for $S(s)$ and $R(s)$, equal to α_{SC}^{-1} and to α_{RC}^{-1} for the sample and reference cells, and equal to the static gain of the compensator (K) in the feedback system. For each component, τ_X indicates the corresponding thermal relaxation time.

Bearing in mind that the feedback system responds much more quickly than the other components of the system, and taking into account that the calorimetric signals are slow, then $\tau_K s \ll 1$; that is to say, the transfer function of the feedback is approximately a constant, $K(s) = K$. With this approximation, it can easily be deduced that the sample cell and the feedback system form a set with a transfer function, $Q(s)$, given by

$$Q(s) = \frac{B}{1 + \tau_Q s}$$

$$\text{with} \quad B = \frac{\alpha_{SC}^{-1}}{1 + K\alpha_{SC}^{-1}}, \quad \tau_Q = \frac{\tau_C}{1 + K\alpha_{SC}^{-1}} \quad (13)$$

As indicated on the right-hand side of the block diagram in Figure 4, the calorimeter is thus reduced to a second-order system. Accordingly, the calorimetric signal can be written in Laplace's domain as

$$\theta(s) = T_{SC}(s) - T_{RC}(s) = G(s)[W_{RX}(s) + W_A(s)] - T_{RC}(s) \quad (14)$$

where $G(s) = S(s)$. $Q(s)$ is the global transfer function for the sample part of the calorimeter, and $W_{RX}(s)$, $W_A(s)$, and $T_{RC}(s)$ are the Laplace transforms of the corresponding time functions. The immediate consequences deriving from the proposed transfer function $G(s)$ are, first, that τ_S is an intrinsic characteristic of the

(16) Calvet, E.; Camia, F. *J. Chem. Phys.* **1985**, *55*, 818−825.
(17) Randzio, S. L.; Sunner, S. *Anal. Chem.* **1978**, *50*, 704−707.
(18) Randzio, S. L.; Suurkuusk, J. Interpretation of Calorimetric Thermograms and their Dynamics Corrections. In *Biological Microcalorimetry*; Beeze, A. E., Ed.; Academic Press: New York, 1980; pp 311−341.
(19) Murray, R. *Spiegel Transformadas de Laplace*; McGraw-Hill: Mexico, 1970.
(20) Kuo, B. C. *Sistemas Automáticos de Control*; ECSA: Barcelona, 1970.
(21) Distefano, J. J.; Stubberud, A. R.; Williams, I. J. *Retroalimentación y sistemas de control*; McGraw-Hill: Mexico, 1972.
(22) López-Mayorga, O.; Mateo, P. L.; Cortijo, M. *J. Phys. E: Sci. Instrum.* **1987**, *20*, 265−269.

sample and is affected only by stirring because the sample is not included in the feedback loop; second, that, to the contrary, the value of τ_Q is modulated with the gain of the feedback loop and thus for a sufficiently high value of K the influence of the term $Q(s)$ can be reduced to the initial instance of the transient response; and third, that the faster response of the instrument results in fewer errors introduced by slow fluctuations of the baseline. In other words, the characteristics of the calorimeter are improved with the compensation of the thermal effect.

Nevertheless, since τ_S is of the same order of magnitude as τ_C, it will not be possible to compensate for all the heat generated in any experiment. The compensation method generates thus two signals, which should be evaluated separately: on one hand, we have the signal corresponding to the compensated heat, Q_c, and on the other, we have that part of the heat that remains without being compensated for, Q_{nc}. The total heat generated in each injection is $Q_{inj} = Q_c + Q_{nc}$, but if the ratio Q_c/Q_{nc} remains constant throughout the experimental measurement range, it would be sufficient to use only one of the two signals. The relationship Q_c/Q_{inj} is constant within experimental error and equal to 0.836 $\pm$ 0.040, which means that approximately 84% of any calorific effect is compensated for and only Q_c (or Q_{nc}) would be necessary to measure the total thermal effects.

Experimental Determination of the Transfer Function of the Calorimeter. With the previous approach, we swapped the problem of solving differential eq 10 for that of determining $G(s)$, so now we set out to determine this global transfer function experimentally.

The response to a heat impulse function, i.e., a heat impulse of infinitesimal duration, has been used to determine the transfer function of isothermal calorimeters.[18,22] Nevertheless, the impulse function is physically unattainable; only if the relaxation time of the chemical reaction is very small and both the injections and the mixing of the reagents are made extremely quickly could the corresponding thermal effect be approximately represented by the response function to a power impulse, i.e., $\delta W(t) = W_0\delta(t)$, where $\delta(t)$ represents the Dirac function and W_0 the pulse amplitude. A more complex but more realistic input function would be a constant power pulse with finite duration. When the thermal effect is generated by an electric heater, the width of this pulse must correspond to the duration of the constant current passed through the heater. For a fast chemical reaction, the width of the pulse must be determined by the time taken to inject and mix the reagent. In any case, the response function to a pulse of duration Δt and power amplitude W_0 can be deduced by considering the input function to be the superimposition of a positive power step over a negative one delayed by Δt: $W(t) = W_0[u(t) - u(t - \Delta t)]$, where $u(t)$ is the unit step function. Another approach to finding the response function is to chop the rectangular heat pulse into n short impulses and try each one as an impulse of infinitesimal duration, $\delta W(t)$.[22−24]

For a calorimeter, the transfer function of which is defined by eqs 13 and 14, the response function to a power pulse of finite duration in the time domain is

$$W(t) = \frac{W_0}{\tau_S - \tau_Q}[\tau_S e^{-(t-\xi)/\tau_S} - \tau_Q e^{-(t-\xi)/\tau_Q} - (\tau_S e^{-\tau/\tau_S} - \tau_Q e^{-\tau/\tau_Q})] \quad (15)$$

where, if $t < \Delta t$, then $\xi = t$, and if $t \geq \Delta t$, then ξ becomes constant and equal to Δt.

We determined the τ_S and τ_Q values experimentally by fitting to eq 15 multiple datasets of electrically generated heats and also those from a protein−ligand interaction reaction and comparing the results. A set of five thermograms (Q1−Q5) from electrically generated, 15-s-wide, heat pulses are shown in the upper plot of Figure 5. The main plot (A) corresponds to the compensated part and the inset (B) to the uncompensated part of the signal. The experimental data are plotted as different symbols, and the solid lines are the thermograms predicted for the parameters indicated in Table 1. In this multiple-dataset-fitting process, the parameter

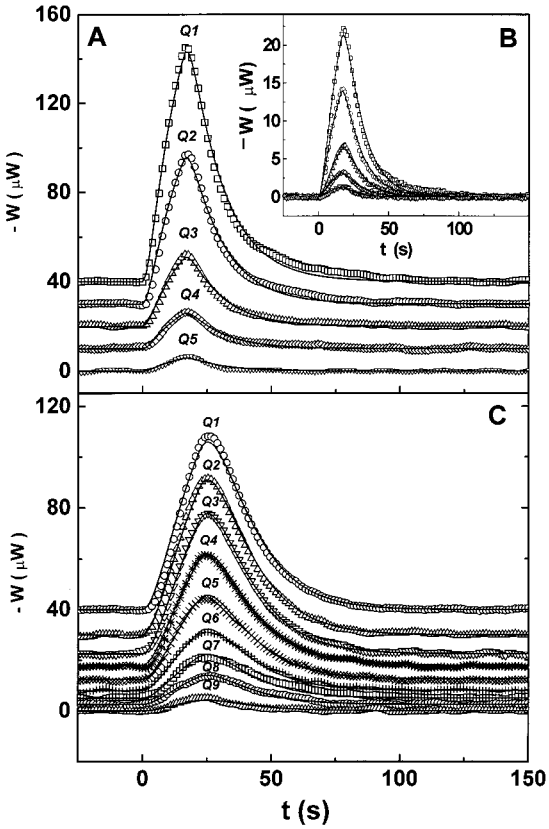

Figure 5. Panels A and B: Five thermograms (Q1−Q5) from electrically generated, 15-s-long heat pulses. The heat values fall in the interval from 130 to 2400 μJ. The main plot (A) corresponds to the compensated part of the total heat and the inset (B) to the noncompensated part. The experimental data are plotted as different symbols, and the solid lines are the thermograms predicted by eq 15, using the parameters indicated in Table 1. Panel C: Nine thermograms (Q1−Q9) corresponding to heat produced when 2′-CMP binds to ribonuclease A in a titration experiment at 0.2 M of ionic strength, consisting of a sequence of 10-μL injections of 2′-CMP. The raw data were treated in similar way to the previous data, except that the effective time of injection and mixing (ϵ) was fixed to 22 s. The parameters resulting from this optimization process are summarized in Table 2.

(23) Löblich, K.-R. *Thermochim. Acta* **1994**, *231*, 7−20.
(24) Löblich, K.-R. *Thermochim. Acta* **1994**, *236*, 39−50.

Table 1. Fitting Parameters for Electrically Generated Heats

dataset[a]	$W_0/(\tau_Q - \tau_S)$ (μW s^{-1})	shared parameters: τ_Q (s)	shared parameters: τ_S (s)
Q_1	14.46 (0.19		
Q_2	9.17 (0.13		
Q_3	4.31 (0.07	13.1 ± 0.1	2.2 ± 0.1
Q_4	2.23 (0.05		
Q_5	0.81 (0.05		

[a] $\chi^2 = 1.2$.

Table 2. Fitting Parameters for the Binding of 2′-CMP to Ribonuclease A

dataset[a]	$W_0/(\tau_Q - \tau_S)$ (μW s^{-1})	shared parameters: τ_Q (s)	shared parameters: τ_S (s)
Q_1	26.23 ± 3.54		
Q_2	24.20 ± 3.27		
Q_3	21.93 ± 2.96		
Q_4	17.41 ± 2.35		
Q_5	13.19 ± 1.78	12.7 ± 0.3	8.8 ± 0.2
Q_6	9.67 ± 1.31		
Q_7	6.89 ± 0.93		
Q_8	4.58 ± 0.62		
Q_9	1.69 ± 0.24		

[a] $\chi^2 = 0.63$.

ξ was fixed at 15 s, and τ_S and τ_Q were shared and were allowed to vary; each dataset had its own value for W_0. A similar treatment was done for a set of peaks corresponding to heat produced when 2′-CMP is bound to ribonuclease A, which is described below. In this case, as the injection and mixing times were not accurately accounted for, a previous fitting, which allowed the parameter ξ to vary, was made in order to optimize its value; this was fixed in the final fitting at 22 s. The parameters resulting from this optimization process are summarized in Table 2.

Interaction of Ribonuclease A and Nucleotides. The binding of nucleotides to ribonuclease A has been extensively studied by microcalorimetry, and, in particular, the binding of the nucleotides 2′-CMP and 3′-CMP, strong competitive inhibitors of the substrate for the active site of the enzyme, has been thermodynamically characterized at different pH values and temperatures.[1,25−28] Thus, these binding reactions seemed to us to be suitable to demonstrate the performance of an isothermal titration microcalorimeter for biological applications. As control experiments, we used the binding of 2′-CMP to bovine pancreatic ribonuclease A under two different solvent conditions, one at the same ionic strength as that used by Wiseman et al.[2] and the other at low ionic strength, for which very different thermodynamic parameters might be expected. The calorimetric study was extended to two other nucleotides, 2′-UMP and 5′-dUMP, the enthalpy changes of which have not been reported in the literature.

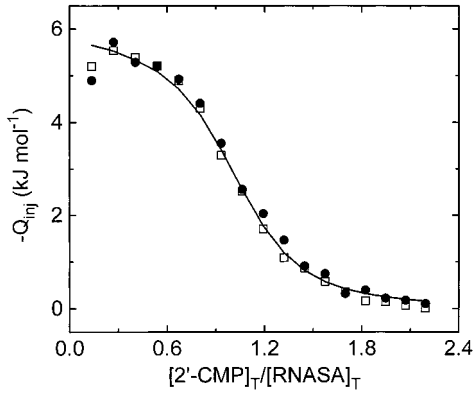

Figure 6. Heat per mole of protein versus total 2′-CMP concentration to the total protein concentration ratio for a calorimetric titration of ribonuclease A with 2′-CMP in NaAc 0.2 M and KCl 0.2 M at pH 5.5 and 25 °C. The symbols ● and □ correspond to two different experiments made under identical conditions; the solid line is that predicted by eq 3 with $m = 1$ and the parameters K and ΔH_b given in Table 3.

Binding of 2′-CMP to Ribonuclease A. A solution of 0.177 mM ribonuclease A at 0.2 M ionic strength was prepared and was assayed as described in the Experimental Section. The injection tube of the sample cell was filled with 2′-CMP solution, and 2.9 mL of protein solution was put into the cell. The reference cell and its injection tube were filled with buffer. Once a stable baseline was reached, a sequence of 18 equivalent 10-μL injections (spaced at 3-min intervals) was begun. The thermal effects associated with protein dilutions were negligible but not so those due to 2′-CMP dilution; thus, the net heats of the binding reaction were obtained by subtracting the dilution heat of 2′-CMP from the total heat generated. The net heats per mole of protein obtained in each injection for two identical experiments are plotted in Figure 6 as a function of the total 2′-CMP concentration to the total protein concentration ratio. The heat associated with the first injection is always less than expected, due to the diffusion of the 2′-CMP during the thermal equilibration time. If a value of 1 is assumed for the number of binding sites, m,[29,30] the thermodynamic parameters obtained by nonlinear least-squares fitting of eq 3 to the experimental data are given in Table 3. $\Delta G°$ and $\Delta S°$ have been calculated by the basic thermodynamic equations $\Delta G° = -RT \ln K$ and $\Delta S° = (\Delta H_b - \Delta G°)/T$.

Using the experimental procedure just described, we carried out a calorimetric titration of ribonuclease A with 2′-CMP at low ionic strength and at 25 °C. The protein and nucleotide solution was prepared in NaAc 50 mM buffer at pH 5.5. A stronger affinity was observed in this binding than in the previous one. In this case, protein saturation was reached at a lower nucleotide concentration, and the titration curve is consequently sharper (result not shown).

Binding of 2′-UMP and 5′-dUMP to Ribonuclease A. In both experiments, the protein was dissolved and dialyzed in NaAc 50 mM at pH 5.5. The protein concentration was 0.29 and 0.22 mM with 2′-UMP and 5′-dUMP, respectively, and the concentrations of 2′-UMP and 5′-dUMP were 8.8 and 11.63 mM, respectively.

(25) Bolen, D. W.; Flogel, M.; Biltonen, R. L. *Biochemistry* **1971**, *10*, 4136−4140.
(26) Flogel, M.; Biltonen, R. L. *Biochemistry* **1975**, *14*, 2603−2609.
(27) Flogel, M.; Biltonen, R. L. *Biochemistry* **1975**, *14*, 2610−2615.
(28) Flogel, M.; Albert, A.; Biltonen R. L. *Biochemistry* **1975**, *14*, 2616−2621.
(29) Allewell, N. M.; Mitsui, Y.; Wyckoff, H. W. *J. Biol. Chem.* **1973**, *248*, 5291−5298.
(30) Weickmann, J. L.; Glitz, D. G. *J. Biol. Chem.* **1982**, *257*, 8705−8710.

Table 3. Apparent Thermodynamic Parameters for the Binding of 2′-CMP, 2′-UMP, and 5′-dUMP to Ribonuclease A at pH 5.5 and 25 °C[a]

ligand	solvent[b]	$K \times 10^{-3}$ (M^{-1})	ΔH_b (kJ mol^{-1})	$\Delta G°$ (kJ mol^{-1})	$\Delta S°$ (J K^{-1} mol^{-1})
2′-CMP	B	112 ± 3	−44.7 ± 0.5	−28.8 ± 0.4	−53.3 ± 0.6
2′-CMP	A	1300 ± 20	−69.1 ± 0.5	−34.9 ± 0.7	−117.7 ± 1.4
2′-UMP	A	145 ± 6	−51.0 ± 1.0	−29.0 ± 2.0	−74.0 ± 3.0
5′-dUMP	A	0.595 ± 0.005	−38.1 ± 2.5	−15.8 ± 1.7	−74.8 ± 0.9

[a] The uncertainties are standard errors in the fitting of the curves. [b] Solvent A, NaAc 50 mM, pH 5.5; solvent B, KAc 0.2 M, KCl 0.2 M, pH 5.5.

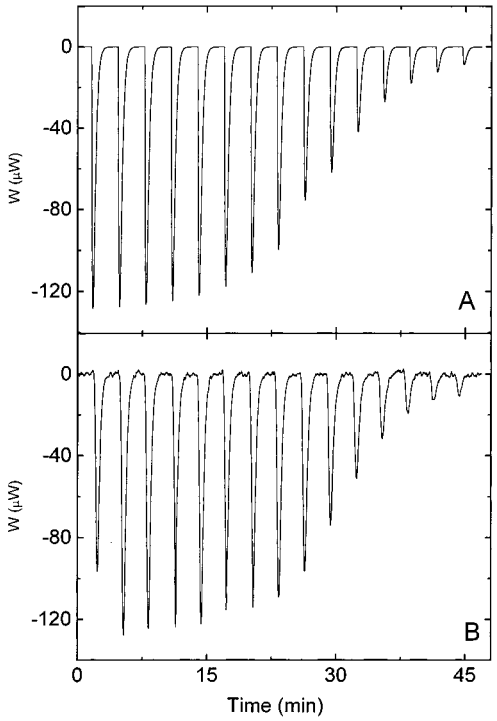

Figure 7. Titration calorimetry of the binding of 2′-UMP to ribonuclease A at 25 °C and pH 5.5. (A)Theoretical thermogram constructed using the total heats calculated for a sequence of 15 10-μL injections of 8.83 mM 2′-UMP on 2.9 mL of 0.191 mM ribonuclease A by the thermodynamic parameters from Table 3. Rectangular power pulses of 22 s with areas equal to the calculated heats were taken as input signals and the output response (thermogram) is calculated using eq 15 and the values given in Table 2 for τ_S and τ_Q. (B) Experimental thermogram obtained under the experimental conditions described in the text.

As in the previous experiments, a number of 10-μL injections of the nucleotide solutions were made into 2.9 mL of the protein solution until a high level of saturation was reached. The temperature was kept at 25 °C. We processed the experimental data in the same way as we did for 2′-CMP binding, and the results are summarized in Table 3.

Figure 7B shows an experimental thermogram of the binding of 2′-UMP to ribonuclease A, and the thermogram predicted by the transfer function is displayed in Figure 7A. To draw this theoretical thermogram, the total heats were calculated for a sequence of 15 equivalent 10-μL injections of 2′-UMP into ribonuclease A, under the experimental conditions already described, using the thermodynamic parameters from Table 3. Thereafter, rectangular pulses of heat power are constructed, the only constraints being that they should be 22 s wide and that the area enclosed by the peaks should correspond to the heats calculated before. Thus, if we take this set of pulses to be the input signal, the output response (thermogram) can be calculated by recourse to eq 15 and the values of τ_S and τ_Q found in Table 2. On comparing the simulated with the experimental thermogram, it can be seen that, except for the first anomalous injection, the form and amplitude of the real peaks are well predicted.

The versatility of this calorimeter is broad in biological systems. Therefore, other calorimetric studies realized are thymidylate synthase with several ligands,[31,32] bovine liver glycogen phosphorylase a and b with adenosine 5′-monophosphate,[33,34] and angiotensin converting enzyme with lisinopril.[35]

CONCLUSIONS

Upon analyzing and comparing the results obtained, we arrive at the three following conclusions: first, the second-order system proposed as a model for our calorimeter seems to be sufficiently correct and valid for any heat conduction isothermal titration. The corresponding transfer function permits the prediction of the response of the instrument in different experiments, equilibrium processes, kinetic processes, and so on with some reliability; second, a time constant of approximately 13 s is maintained, and it would seem reasonable to assign this value to the cell sensor device common to both experiments; and third, the other time constant for the binding reaction is 4 times higher than that corresponding to the electrical heats, which is to be expected since the heat transfer from the electric heater to the cell sensor device is faster than heat conduction through an aqueous reacting solution with lower thermal diffusivity and that it is not instantaneously mixed.

The thermodynamic parameters for the binding of 2′-CMP to ribonuclease A agree within experimental error with those published.[2] A similar dependence of the binding parameters upon ionic strength was observed for the binding of the 3′-CMP.[25] These results confirm the validity of the calorimeter system for the study of biochemical reactions.[31−35]

The association constant obtained for the 2′-UMP nucleotide agrees well with the value already published,[36] and, as with other nucleotides, the binding process is enthalpy driven and has an

(31) García-Fuentes, L.; Reche, P.; López-Mayorga, O.; Santi, D. V.; González-Pacanowska, D.; Barón, C. *Eur. J. Biochem.* **1995**, *232*, 641−645.
(32) Téllez-Sanz, R.; Bernier-Villamor, V.; García-Fuentes, L.; González-Pacanowska, D.; Barón, C. *FEBS Lett.* **1997**, *409*, 385−390.
(33) García-Fuentes, L.; Cámara-Artigas, A.; López-Mayorga, O.; Barón, C. *Biochim. Biophys. Acta* **1996**, *1294*, 83−88.
(34) García-Fuentes, L.; Cámara-Artigas, A.; López-Mayorga, O.; Barón, C. *J. Biol. Chem.* **1996**, *271*, 27569−27574.
(35) Téllez-Sanz, R.; García-Fuentes, L.; Barón, C. *FEBS Lett.* **1998**, *423*, 75−80.

unfavorable change of entropy. On comparing the results for the 2′-UMP and 5′-dUMP nucleotides, we can detect a notable difference in the association constant, the affinity of 5′-dUMP being somewhat lower; a similar difference has been found between the affinities of 2′-CMP and 5′-dCMP for ribonuclease A.[36] The entropy changes for these two nucleotides are practically the same, which seems to suggest that the origin of this affinity difference is in the enthalpy change.

ACKNOWLEDGMENT

We thank the Biocalorimetry Center of The Johns Hopkins University (JHU) for constructing the calorimetric cells and Dr. E. Freire from the JHU Biology Department for his useful advice. This research was supported by Grants PB96-1446 and PM97-0003 from DGICYT, Ministerio de Educación y Ciencia, Spain.

SUPPORTING INFORMATION AVAILABLE

Design of the calorimeter cells, design and position of the electrical calibration heater, and design of the stirrer and injection device (7 pages). See any current masthead page for ordering information.

Received for review February 23, 1998. Accepted August 19, 1998.

AC980203U

(36) Eftink, M. R.; Biltonen, R. L. Pancreatic ribonuclease A: the most studied endoribonuclease. In *Hydrolytic Enzymes*; Neuberger, A., Brocklehurst, K., Eds.; Elsevier Science Publishers B.V. (Biomedical Division): Amsterdam, 1987; Vol. 16, pp 333−376.